KONA Powder and Particle Journal

KONA Powder and Particle Journal No. 42 (2025) 261–267/https://doi.org/10.14356/kona.2025015 Original Research Paper

Compression of an Assembly of Bi-Dispersed Particles †

Ching S. Chang [1]*, Jason Chao [1] and Yibing Deng [2]

[1] *Department of Civil and Environmental Engineering, University of Massachusetts, USA*
[2] *Shanghai Urban Construction Vocational College, China*

A compression model that elucidates the compressibility of a granular soil assembly is useful for engineering and mechanical applications. While the literature offers numerous compressibility models for granular soils, a significant limitation arises because these models overlook the impact of soil composition. Typically, soils consist of a blend of sand and silt as a result of geological processes. Moreover, empirical observations indicate a substantial influence of silt content on the compressional behavior of bi-dispersed granular soils. This study introduces an approach grounded in a more rigorous theoretical foundation for predicting the compression of bi-dispersed packings. The analytical method is based on Edwards thermodynamics, which is a realm of physics. Within this framework, the analytical method incorporates the excess free volume resulting from the dispersity of the bi-dispersed particle packing. An evaluation was conducted to validate the model's applicability by comparing the predictions with the experimental results for Hokksund sand-silt mixtures.

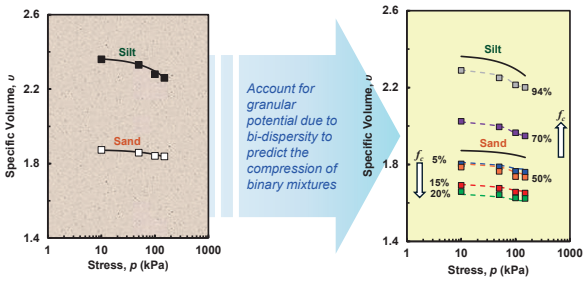

Keywords: compression, powder, particle, thermodynamics, bi-dispersed packing

1. Introduction

The soil compressibility is a vital engineering property that critically influences optimizing design protocols and comprehensive assessments. A compression model that elucidates the relationship between stress and void ratio is very useful for analyzing soil foundations or earth structures (Lehane and Fahey, 2002) and is also an essential component of critical state soil mechanics.

Numerous compressibility models for granular soils have been proposed (Chong and Santamarina, 2016; Hardin, 1987; Meidani et al., 2017; Pestana and Whittle, 1995; Schofield and Wroth, 1968; Vesić and Clough, 1968). These models typically use empirical methodologies that incorporate initial density, soil type, and applied stress. However, a notable drawback exists in these models, as they neglect the impact of soil composition. This oversight is significant because natural soils or man-made fills typically comprise a combination of sand and silt due to geological processes such as erosion, breakage, and weathering. Furthermore, it has been observed that the fractional content of silt (fines content f_c) has a substantial influence on the compressional behavior of granular soils in experiments (Carrera et al., 2011; Konishi et al., 2007; Lipiński et al., 2017; Lupogo, 2009; Xu et al., 2009; Yang et al., 2006; Zuo and Baudet, 2020) and in discrete element simulations (Minh et al., 2014; Wiącek et al., 2017). Thus, a comprehensive understanding of the effects of fines content is essential for engineers when assessing the deformation characteristics of granular soils. It is highly desirable to have a model that explicitly accounts for the effect of fines content on compressibility.

The current literature offers only a limited number of approaches for examining how the fines content influences the compressional behavior of sand-silt mixtures. Thevanayagam et al. (2002) introduced the concept of the intergranular void ratio for a sand silt mixture, while Cabalar and Hasan (2013) and Monkul and Ozden (2007) empirically correlated the intergranular void ratio with compressibility. Chang et al. (2017) proposed a compression model for sand-silt mixtures, in which a parameter is empirically determined as a function of fines content.

In this study, we propose an approach with a more rigorous theoretical foundation for predicting the compression of a sand-silt mixture. The analytical method was based on Edwards thermodynamics for granular materials. Within this framework, we hypothesized that the presence of excess free-volume potential in bi-dispersed particle packing (Chang, 2022a) is similar to the excess free energy observed in chemical solutions containing two species of molecules. Using this concept, we modeled the compressibility of binary mixtures of granular soil with varying fines content, considering the potential of excess free volume to cause additional volume reduction during compression.

† Received 7 May 2024; Accepted 3 July 2024
J-STAGE Advance published online 10 August 2024
* Corresponding author: Ching S. Chang;
Add: 130 Natural Resources Road, Marston Hall, Amherst, MA 01003, USA
E-mail: chang@ecs.umass.edu
TEL: +1-413-545-5401

In the subsequent sections, we first briefly describe the concept of excess free volume and define a granular potential related to the volume change in a bi-dispersed packing. Then, the compression model framework was formulated considering the granular potential of a bi-dispersed packing. To validate our proposed model, we compared the predicted outcomes with the experimental results for Hokksund sand-silt mixtures. The effect of the fines content on the compressibility is discussed, and the applicability of the model is highlighted.

2. Modeling concept

The decrease in volume due to packing compression typically involves two main aspects: (1) the elastic deformation of solid particles, and (2) the reduction of void volume resulting from particle rearrangement, which is treated as plastic deformation in an elastic-plasticity framework. As the magnitude of elastic deformation is typically minimal, this investigation disregards it, and compressibility is only considered due to the rearrangement of particles under stress. This rearrangement reduces the number of voids among particles, thereby decreasing the void ratio.

Here, we focus solely on bi-dispersed packings. The void ratio is assumed to be influenced by two main variables: $e(p, y_2)$, where y_2 is the solid fraction of fine particles (note: the solid fraction of coarse particles $y_1 = 1 - y_2$ in a bi-dispersed mixture).

2.1 Compression of bi-dispersed packing

For a mono-dispersed packing assembly comprising N particles, the total assembly volume V is given by $V = v^o N$. Here, v^o is termed particle volume, representing the average volume of a solid particle and its surrounding void space. The magnitude of v^o is dependent on the density and the applied pressure of the packing.

In the case of bi-dispersed packing, the total granular system volume $V = v_1N_1 + v_2N_2$. Here, N_1 and N_2 are number of particles in species 1 and 2, respectively; v_1 and v_2 are the partial particle volumes associated with species 1 and 2, respectively.

We note that under the same applied pressure and relative density, the particle volume v_i^0 in a mono-dispersed packing differs from the partial particle volume v_i in a bi-dispersed packing. The change in volume from v_i^0 to v_i arises from particle interactions due to the mixing of two species.

This phenomenon resembles the change in mole energy observed in mixed chemical solutions, which results from the interaction between two species of molecules. Analogous to free energy in thermodynamics, we consider the concept of "free volume," representing the available void volume in a packing that can be changed during particle rearrangement.

Thus, we adopt an approach akin to the "Gibbs excess free energy" concept in classic thermodynamics (Silbey et al., 2004). In this context, we define the *excess free volume* Δv_i of each species as

$$v_i = v_i^0 - \Delta v_i \tag{1}$$

In conventional usage, "excess free energy" typically denotes the additional energy available for performing work resulting from chemical reactions among multiple species (Silbey et al., 2004). However, in this case, the *excess free volume* Δv_i represents the extra volume available for reduction due to the size difference between the two particle species.

From **Eqn. (1)**, we observe that the difference between the monoparticle volume and partial particle volume (i.e., $v_i^0 - v_i$) signifies the volume reduction potential of each species. In a mixture of two species, the excess free volume of both species is diminished, resulting in a reduction in the overall volume of the packing mixture.

2.2 Excess free volume

To quantify the excess free volume in each species, we determined the partial particle volumes v_1 and v_2. For a bi-dispersed packing, the total granular system volume V is an extensive variable and is homogeneous of degree 1 (Silbey et al., 2004); thus, according to Euler's homogeneous function theorem, the total volume of a mixture is given by

$$V(N_1, N_2) = \frac{\partial V}{\partial N_1} N_1 + \frac{\partial V}{\partial N_2} N_2 = v_1 N_1 + v_2 N_2 \tag{2}$$

This relationship is critical because it reveals how the partial particle volumes are related to the partial derivative with respect to the number of particles in each species, providing a central understanding for estimating their values.

Using a statistical mechanics approach, we represent the global packing configuration as a set of microstates. Each microstate is a local configuration of a single particle and its nearest neighbors. Using this model, we analyze the values of partial particle volumes v_1 and v_2.

Eqn. (2) provides a method for measuring the partial particle volume of a species. The partial particle volume v_1 can be defined as $\partial V/\partial N_1$, where the change in assembly volume $\mathrm{d}V$ is caused by adding a small number ($\mathrm{d}N_1$) of large particles to the mixture while keeping the total number N_2 of small particles constant. The partial particle volume v_2 can be determined similarly.

To consider the local configuration, we deliberately considered a single particle added to the mixture at a random location. By repeating the process M times, we obtain M different local configurations for the added particle and its neighboring particles. Then, this statistical mechanics approach can be employed to obtain the value of $\partial V/\partial N_1$ from this set of local configurations.

However, directly determining v_1 and v_2 through statistical mechanics is challenging due to the lack of detailed knowledge about the complete packing structure, which makes it impractical to generate all possible microstates of the system. Nevertheless, this concept can help us estimate the possible ranges of v_1 and v_2 by analyzing the following extreme scenarios of microstates.

(1) Inserting a large particle:

a) If the surrounding particles are all large, as shown in **Fig. 1(a)**, the added particle displaces them, increasing the packing volume. This scenario is akin to a uniformly sized packing; thus, the volume change ΔV is comparable to the baseline particle volume v_1^0. Thus, $v_1 = v_1^0$ and the excess free volume is zero.

b) Conversely, if the surrounding particles are all small (**Fig. 1(b)**, the void volume around the added large particle varies with the sizes of the neighboring particles. When the large particle is surrounded by tiny particles, the void volume is minimized. In this case, ΔV is similar to the volume of the solid particle v_1^g, hence $v_1 = v_1^g$, and the excess free volume is $\left(v_1^0 - v_1^g\right)$.

Considering both extreme scenarios, the possible range of excess free volume for the large-particle species was determined to range from 0 to $\left(v_1^0 - v_1^g\right)$.

(2) Inserting a small particle:

a) When all surrounding particles are small, as shown in **Fig. 1(c)**, the local configuration resembles uniform packing. The volume change ΔV due to inserting the small particle is similar to the baseline particle volume v_2^0, thus $v_2 = v_2^0$, and the excess free volume is zero.

b) Conversely, if the surrounding particles are all large, as shown in **Fig. 1(d)**, and the inserted particle is significantly smaller than the available void space, it remains mobile despite the surrounding particles being jammed (mechanically stable). This particle is called a rattler particle. In this scenario, the change in system volume ΔV is negligible, so $v_2 = 0$, and the excess free volume is v_2^0.

Considering both extreme scenarios, the possible excess free volume for the small-particle species was determined to range from 0 to v_2^0.

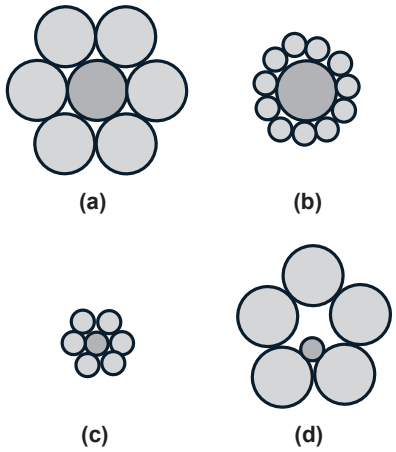

Fig. 1 Four extreme scenarios: **(a)** a large particle surrounded by large particles, **(b)** a large particle surrounded by small particles, **(c)** a small particle surrounded by small particles, and **(d)** a small particle surrounded by large particles.

2.3 Determination of granular potential

For convenience, we express the excess free volume as a dimensionless variable. The granular potential μ_i of the ith species was defined as excess free volume per unit solid volume, i.e., $\mu_i = \Delta v_i / v_i^g$.

In this context, all volumes are replaced by specific volumes. **Eqn. (1)** becomes $\upsilon_i = \upsilon_i^0 - \mu_i$, where υ_i^0 is the specific volume of the ith mono-dispersed packing, and μ_i is the granular potential. And **Eqn. (2)** can be written as

$$\upsilon = \upsilon_1 y_1 + \upsilon_2 y_2 \tag{3}$$

Here, y_1 and y_2 are the solid fractions of the large and small particles, respectively.

By using **Eqn. (3)** and $\upsilon_i = \upsilon_i^0 - \mu_i$, it can be expressed as

$$\upsilon = \sum_{i=1}^{2} \upsilon_i^0 y_i - \sum_{i=1}^{2} \mu_i y_i \tag{4}$$

Note that, **Eqn. (4)** delineates the free volume into two components: the first term represents the volume average of the two components, representing the volume without particle interactions between the two species, and the second term represents the volume reduction due to the release of granular potential from the interaction between the two species. The second term is also defined as the Gibbs volume potential given by

$$G = \mu_1 y_1 + \mu_2 y_2 \tag{5}$$

Based on the previous analysis, the range of the granular potential μ_1 extends from 0 to $(\upsilon_1^0 - 1)$, while the range of μ_2 spans from 0 to υ_2^0. This can be expressed as follows:

$$\mu_1 = \alpha_1(\upsilon_1^0 - 1); \quad \mu_2 = \alpha_2 \upsilon_2^0 \tag{6}$$

Here both $0 < \alpha_1 < 1$ and $0 < \alpha_2 < 1$. The specific values of α_1 and α_2 are dependent on the nature of the interactions between species, which are influenced by the overall structure and composition of the assembly.

To determine the values of α_1 and α_2, we assume variables α_1 and α_2 are functions of the characteristic length λ introduced for the bi-dispersed packing, falling within the range $d_1 \geq \lambda \geq d_2$. The variable λ is an internal variable whose value depends on the overall structure and composition of the assembly.

As elucidated by Chang (2022a), in the context of particle filling and embedment mechanisms, the expressions of granular potential for the two species are given as follows:

$$\mu_1 = (v_1^0 - 1)\left(1 - \frac{\lambda}{d_1}\right)^{\eta}; \quad \mu_2 = v_2^0\left(1 - \frac{d_2}{\lambda}\right)^{\eta} \tag{7}$$

It is important to note that, in **Eqn. (4)**, when the second term (granular potential) is zero, for the example of the size ratio between the two species equaling 1 (i.e., $\lambda = d_1 = d_2$, see **Eqn. (7)**), the specific volume versus fines content f_c forms a line identical to the line $v_1^0 y_1 + v_2^0 y_2$ shown in **Fig. 2**, which represents the upper bound for the granular mixture with zero interactions between species.

Conversely, when the size ratio approaches infinity ($d_2 \ll d_1$), the predicted relationship is illustrated in **Fig. 2** by two lines AB and BC, which respectively represent the lower bounds of the granular mixture. For the range AB, $\lambda = d_1 \gg d_2$, **Eqn. (7)** shows that $\mu_1 = 0$, and $\mu_2 = v_2^0$. The equation of AB is $(v_1^0 y_1 + v_2^0 y_2) - v_2^0 y_2$. For the range BC, $\lambda = d_2 \ll d_1$, **Eqn. (7)** shows that $\mu_2 = 0$, and $\mu_1 = v_1^0 - 1$. The equation of BC is given by $(v_1^0 y_1 + v_2^0 y_2) - (v_1^0 - 1) y_2$.

The curve with symbols in **Fig. 2** represents measured specific volumes for the Hokksund sand-silt mixture. At f_c = 20 %, the granular potential G calculated from **Eqn. (5)** is the distance from the upper bound line to the measured curve. In general, considering the overall structure and composition of the assembly, the granular potential of a packing lies between the upper bound and the lower bound, as calculated from **Eqn. (7)** using the values of λ and η. The exponents η is a material constant that depends on the shape and surface friction of particles and can be calibrated from the measured volume of one specimen with a particular fines content f_c (Chang, 2022a,b).

The characteristic length λ can be determined by the second law of thermodynamics. In the case of Edwards thermodynamic theory, the second law of thermodynamics stipulates that the Gibbs volume potential must be minimized for a closed system to reach equilibrium at constant compactivity (Chang, 2022b). Since the parameters e_1^0, d_i, y_i, η are constant, the following condition holds.

$$\frac{dG}{d\lambda} = \frac{d}{d\lambda}\left(\mu_1(v_1^0, \lambda) y_1 + \mu_2(v_2^0, \lambda) y_2\right) = 0 \tag{8}$$

The two terms in this equation can be regarded as the volume transfers between the two species, and their zero-sum ensures the condition of steady-state volume at equilibrium. This characteristic allows us to determine the value of λ, thus to calculate the granular potentials μ_i for each species. Consequently, this principle provides a straightforward method for predicting the specific volume of a mixture based on the specific volumes of its individual components.

This theory's validity has been confirmed by verifying the maximum and minimum void ratios through ASTM compacted procedures for soil mixtures of various types (Chang, 2022b).

To illustrate the prediction process, an example of a Hooksund sand-silt mixture is used, where the silt volume fraction y_2 = 0.2. The sand particles were 0.45 mm in size, while the silt particles were 0.032 mm. At a pressure of 10 kPa, the specific volume for sand is v_i^0 = 1.873, and for silt, it's v_2^0 = 2.36.

We initially assumed a trial value of η = 3.6. The Gibbs volume potential G of the packing (see **Eqns. (5)** and **(7)**) was calculated for the range $0.45 \geq \lambda \geq 0.032$ as shown in **Fig. 3**. The minimum of G corresponds to λ = 0.2637. At this value of λ, $\mu_1 y_1$ = 0.029 for sand particles and $\mu_2 y_2$ = 0.296 for silt particles. The volume reduction potential was G = 0.325.

The specific volume of the mixture can then be obtained in **Eqn. (4)**. With $v_1^0 y_1 + v_2^0 y_2 = 1.9704$ and G = 0.325, the calculated specific volume for the bi-dispersed packing at fines content f_c = 0.2 is 1.6504 (i.e., 1.9704 − 0.325).

If the predicted value does not match the measured value, the value of η can be calibrated. Once the correct value of η is determined, it can be used to predict specific volumes for any other fines content. The calculated curve is plotted as a solid line in **Fig. 2** and compared with the measured results represented by symbols.

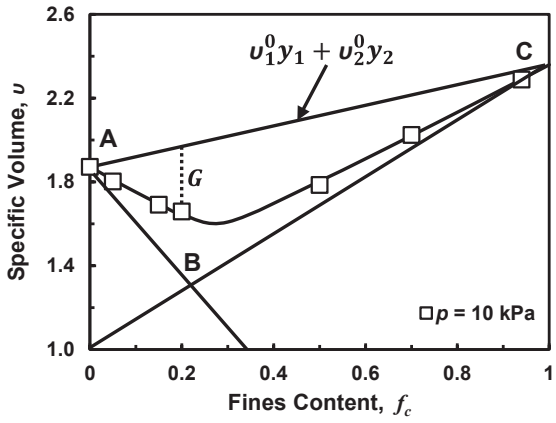

Fig. 2 The specific volume versus fines content. The line of AC is the upper bound, and the line of ABC is the lower bound of granular potential. Adapted with permission from Ref.(Yang et al., 2006). Copyright: (2006) ASTM International.

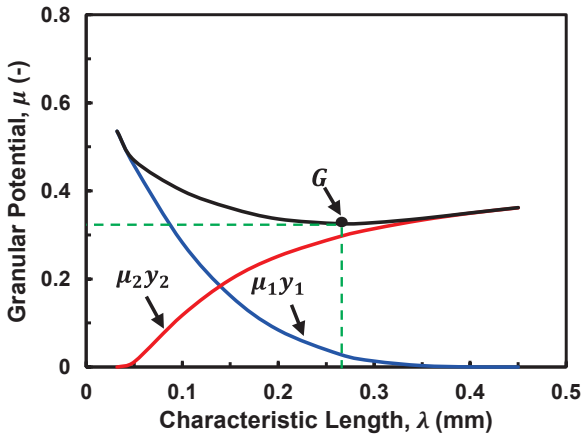

Fig. 3 Calculated granular potential of each species and Gibbs volume potential for the bi-dispersed packing.

3. Experimental data

To verify the proposed model for soil mixtures under static load compression, we selected experiments on the sand-silt mixtures reported by Yang et al. (2006). These experiments involve various particle size combinations. For the mixtures, the mean sizes (d_{50}) of the sand and silt particles were 0.45 mm and 0.032 mm, respectively, resulting in a particle size ratio of 14. The soil mixtures were composed of Hokksund sand and nonplastic Chenbei silt. Samples were prepared with fines contents ranging from 5 % to 94 %. All samples were prepared using moisture tamping to achieve a relative density (D_r) of 20 %. This ensured that the observed difference in compressibility of the samples was due to the fines content of the soil mixture and not the relative density.

During compression testing, samples were subjected to isotropic loading up to 200 kPa. At this stress level, no evidence of particle crushing was observed in the compression experiments, ensuring that the fines content remained constant throughout each test.

4. Results

To understand how static compression affects bi-dispersed packing, we modify **Eqn. (4)** to accommodate pressure-dependent functions for both v_i^0 and μ_i. The modified equation is expressed as follows:

$$v = \sum_{i=1}^{2} v_i^0(p)\, y_i + \sum_{i=1}^{2} \mu_i\left(v_i^0(p), f_c\right) y_i \tag{9}$$

In this equation, $v_i^0(p)$ represents the individual compression behavior of the two components of the mixture. $\mu_i\left(v_i^0(p), f_c\right)$ represents the volume reduction due to the impact of the granular potential resulting from the bi-dispersity of the assembly.

In **Eqn. (9)**, the granular potential μ_i is a function of $v_i^0(p)$ dependent on applied stress p. Once $v_i^0(p)$ is known, the evolution of granular potential μ_i can be obtained from **Eqns. (7)** and **(8)** following the previously described process.

The expression of $v_i^0(p)$ can be obtained from the individual compression curves of the sand and silt using any phenomenologically based analytical model.

4.1 Compression of monodispersed packing

In **Fig. 4**, the two compression curves of sand and silt, which are the components of the Hokksund sand-silt mixture, are displayed as symbols. The sand and silt particle assemblies were compacted to the same relative density (D_r = 20 %). We adopted the compression model proposed by Meidani et al. (2017) to obtain the expressions for the two compression curves.

In this model, the total volume of voids is conceptually divided into two fractions: (1) active void volume, which is subject to reduction and eventual elimination through particle rearrangement, and (2) inactive void volume within interlocked particles, which cannot be further reduced by particle rearrangement.

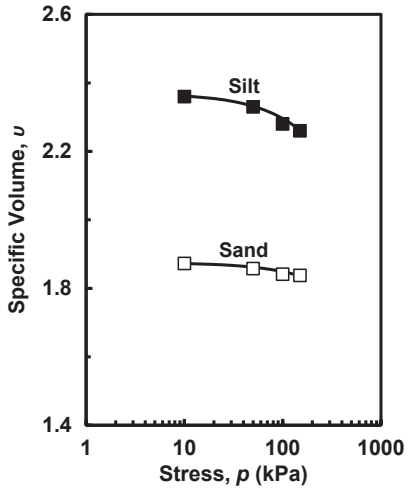

Fig. 4 Comparison of predicted and measured compression curves for sand and silt of the Hokksund sand-silt mixture. Adapted with permission from Ref.(Yang et al., 2006). Copyright: (2006) ASTM International.

Meidani et al. (2017) observed that the variation of ($\mathrm{d}v$/$\mathrm{d}p$) versus v exhibits linear relationship for several types of sand and silt. The linear relationship can be expressed as follows:

$$\frac{\mathrm{d}v}{\mathrm{d}p} = \alpha\left(v - v_r\right) \tag{10}$$

The parameter v_r represents the inactive part of the specific volume. Let a dimensionless parameter $a = \alpha p_a$, and the integral of this equation becomes

$$v(p, v_0) = \left[v_0 - v_r\right]\exp\left(-\frac{a}{p_a}p\right) + v_r \tag{11}$$

Here v_0 is the initial specific volume, p is the applied pressure, and p_a is the atmospheric pressure (101.325 kPa). The model relies on two parameters a and v_r, with v_r being the inactive specific volume of the packing and a is a material constant.

In **Fig. 4**, **Eqn. (11)** is used to model the compression curves of the sand and silt. For the sand compression curve, the parameters $v_0 = 1.873$, $v_r = 1.48$, and $a = 0.0611$ are employed, while for the silt compression curve, the parameters $v_0 = 2.360$, $v_r = 1.55$, and $a = 0.0611$ are used. The modeled curves are represented by solid lines, and the measured results are plotted as symbols.

4.2 Compression of bi-dispersed packing

In **Fig. 5**, the measured compression data for Hokksund sand-silt mixtures with fines contents ranging from 5 % to 94 % (f_c = 5, 15, 20, 50, 70, and 94 %) are presented as symbols. The influence of the fines content on the

compression curves can be observed from two perspectives: the initial specific volumes and the shape of the compression curves.

At an initial confining pressure of 10 kPa, significant variations were observed in the initial specific volumes for bi-dispersed specimens with different fines contents.

The trend shows that the initial specific volume decreases as the fines content increases up to 20 %, which is caused by the filling of voids between sand particles by silt particles. At a 20 % fines content, the voids between sand particles were nearly filled. Consequently, further increases in fines content beyond 20 % caused the additional silt particles to separate and lose contact, reversing the volume decrease trend and leading to an increase in volume.

These initial specific volumes for all fines contents are shown in **Fig. 5**, which were previously predicted and plotted in **Fig. 2**. The parameter $\eta = 3.6$ was calibrated from the data point at $p = 10$ kPa and $f_c = 0.2$.

The shape of the compression curve can be computed using **Eqn. (9)**. The analytical expressions of the compression curves of sand ($v_i^0(p)$) and silt ($v_2^0(p)$) serve as input information for predicting the compression curves of sand-silt mixtures. With these two functions, the granular potential μ_i can be obtained from **Eqns. (7)** and **(8)**. The required parameters for predicting the compression curves are summarized as follows:

- To simulate $v_i^0(p)$ for sand: $v_r = 1.48$, $a = 0.0611$.
- To simulate $v_2^0(p)$ for silt: $v_r = 1.55$, $a = 0.0611$.
- To calculate granular potential μ_i: $\eta = 3.6$.

The methods for determining v_r and a are described in **Section 4.1**, and the method for determining η is described in **Section 2.3**.

In **Fig. 5**, the two solid lines represent the predicted compression curves of the sand and silt (replotted from **Fig. 4**). The predicted curves for mixtures with different fines content are depicted by dashed lines and are compared with the measured data points represented by symbols. The fines content for each compression curve is indicated on the left or right side of the curve. Initially, the compressibility of the mixture decreases with increasing fines content. However, after reaching 20 % fines content, the trend reversed, and the compressibility increased with further increasing fines content.

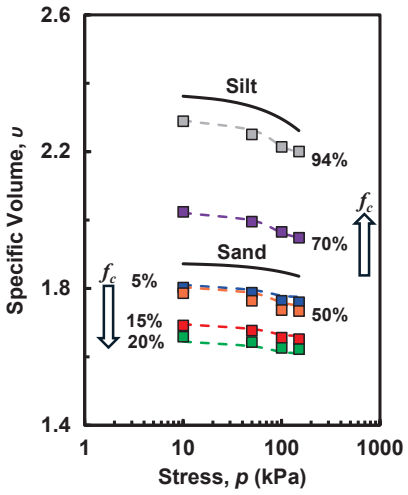

Fig. 5 Comparison of predicted and measured compression curves for the Hokksund sand-silt mixtures with various fines contents. Adapted with permission from Ref. (Yang et al., 2006). Copyright: (2006) ASTM International.

5. Conclusion

The fines content significantly influences the compressibility of bi-dispersed packing. To address this influence, we developed an analytical model grounded in a physics-based methodology for predicting the compression of such mixtures. The proposed model effectively explains the significant variation in the initial specific volume of specimens after compression. Furthermore, it accurately captures the compressibility patterns under various compression loads in soil mixtures with diverse fines contents. Consequently, the notion of granular potential stemming from bi-dispersity emerges as a credible framework for modeling the assembly of bi-dispersed particles. It is worth noting that this model is applicable only to mixtures of dry particles with particle sizes greater than 2 μm. The effects of hydration, capillary, and cohesive forces exhibit in wet particles are not considered.

Acknowledgments

This work was supported by the National Science Foundation of US under the research grant CMMI-1917238.

Data Availability Statement

Data on compression curves for sand and silt of the Hokksund sand-silt mixture are available publicly in J-STAGE Data (https://doi.org/10.50931/data.kona.27139746).

Nomenclature

d_i	particle size (mm)
d_{50}	the mean particle size (mm)
D_r	relative density (-)
e	void ratio (-)
e_i^0	void ratio of mono-dispersed species (-)
f_c	fines content (solid fraction of small particles)
G	Gibbs volume potential (-)
N_i	number of particles in the ith species (-)
p	applied pressure (Pa)
v_i	partial particle volume of *the* ith species (mm^3)
v_i^0	particle volume of the *the* ith species (mm^3)
v_i^g	volume of a solid particle of the ith species (mm^3)
Δv_i	the excess free volume of *the* ith species (mm^3)
V	total assembly volume (mm^3)
V_s	solid volume (mm^3)
y_i	solid volume fraction of the ith species (-)
λ	characteristic length (mm)
μ_i	granular potential of the ith species (-)

v specific volume (-)
v_0 initial specific volume (-)
v_i partial specific volume of the *i*th species (-)
v_i^0 specific volume of *the i*th species (-)
v_r inactive specific volume (-)
η material constant (-)

References

Cabalar A.F., Hasan R.A., Compressional behaviour of various size/shape sand-clay mixtures with different pore fluids, Engineering Geology, 164 (2013) 36–49. https://doi.org/10.1016/j.enggeo.2013.06.011

Carrera A., Coop M., Lancellotta R., Influence of grading on the mechanical behaviour of Stava tailings, Géotechnique, 61 (2011) 935–946. https://doi.org/10.1680/geot.9.P.009

Chang C.S., Jamming density and volume-potential of a bi-dispersed granular system, Geophysical Research Letters, 49 (2022a) e2022GL098678. https://doi.org/10.1029/2022GL098678

Chang C.S., Deng Y., Compaction of bi-dispersed granular packing: analogy with chemical thermodynamics, Granular Matter, 24 (2022b) 58. https://doi.org/10.1007/s10035-022-01219-5

Chang C.S., Meidani M., Deng Y., A compression model for sand–silt mixtures based on the concept of active and inactive voids, Acta Geotechnica, 12 (2017) 1301–1317. https://doi.org/10.1007/s11440-017-0598-1

Chong S.-H., Santamarina J.C., Soil compressibility models for a wide stress range, Journal of Geotechnical and Geoenvironmental Engineering, 142 (2016) 06016003. https://doi.org/10.1061/(ASCE)GT.1943-5606.0001482

Hardin B.O., 1-D Strain in normally consolidated cohesionless soils, Journal of Geotechnical Engineering, 113 (1987) 1449–1467. https://doi.org/10.1061/(ASCE)0733-9410(1987)113:12(1449)

Konishi Y., Hyodo M., Ito S., Compression and undrained shear characteristics of sand-fines mixtures with various plasticity, Doboku Gakkai Ronbunshuu C, 63 (2007) 1142–1152. https://doi.org/10.2208/jscejc.63.1142

Lehane B., Fahey M., A simplified nonlinear settlement prediction model for foundations on sand, Canadian Geotechnical Journal, 39 (2002) 293–303. https://doi.org/10.1139/T01-091

Lipiński M.J., Wdowska M.K., Jaroń Ł., Influence of fines content on consolidation and compressibility characteristics of granular materials, IOP Conference Series: Materials Science and Engineering, 245 (2017) 032062. https://doi.org/10.1088/1757-899X/245/3/032062

Lupogo K., Effects of fines on mechanical behaviour of sandy soils, master thesis, Delft University of Technology, (2009). <https://repository.tudelft.nl/record/uuid:f4b5b6d0-8b00-44da-8011-cd664bfa96bd>accessed05072024.

Meidani M., Chang C.S., Deng Y., On active and inactive voids and a compression model for granular soils, Engineering Geology, 222 (2017) 156–167. https://doi.org/10.1016/j.enggeo.2017.03.006

Minh N.H., Cheng Y.P., Thornton C., Strong force networks in granular mixtures, Granular Matter, 16 (2014) 69–78. https://doi.org/10.1007/s10035-013-0455-3

Monkul M.M., Ozden G., Compressional behavior of clayey sand and transition fines content, Engineering Geology, 89 (2007) 195–205. https://doi.org/10.1016/j.enggeo.2006.10.001

Pestana J.M., Whittle A.J., Compression model for cohesionless soils, Geotechnique, 45 (1995) 611–631. https://doi.org/10.1680/geot.1995.45.4.611

Schofield A.N., Wroth C.P., Critical State Soil Mechanics, McGraw-Hill, Maidenhead, England, 1968, ISBN: 978-0070940482.

Silbey R.J., Alberty R.A., Bawendi M.G., Physical Chemistry, 4th edition, Wiley, 2004, ISBN: 978-0471215042.

Thevanayagam S., Shenthan T., Mohan S., Liang J., Undrained fragility of clean sands, silty sands, and sandy silts, Journal of Geotechnical and Geoenvironmental Engineering, 128 (2002) 849–859. https://doi.org/10.1061/(ASCE)1090-0241(2002)128:10(849)

Vesić A.S., Clough G.W., Behavior of granular materials under high stresses, Journal of the Soil Mechanics and Foundations Division, 94 (1968) 661–688. https://doi.org/10.1061/JSFEAQ.0001134

Wiącek J., Parafiniuk P., Stasiak M., Effect of particle size ratio and contribution of particle size fractions on micromechanics of uniaxially compressed binary sphere mixtures, Granular Matter, 19 (2017) 34. https://doi.org/10.1007/s10035-017-0719-4

Xu M., Song E.X., Cao G., Compressibility of broken rock-fine grain soil mixture, Geomechanics and Engineering, 1 (2009) 169–178. https://doi.org/10.12989/gae.2009.1.2.169

Yang S.L., Lacasse S., Sandven R., Determination of the transitional fines content of mixtures of sand and non-plastic fines, Geotechnical Testing Journal, 29 (2006) 102–107. https://doi.org/10.1520/GTJ14010

Zuo L., Baudet B.A., Normalised behaviour of a non-plastic silt–pumice sand mixture, Géotechnique, 70 (2020) 822–832. https://doi.org/10.1680/jgeot.19.P.012

Authors' Short Biographies

Prof. Ching S. Chang is a Professor of Civil and Environmental Engineering at the University of Massachusetts, Amherst. With over 30 years of experience, he specializes in multi-scale modeling and the constitutive behavior of granular soils, clay, asphalt concretes, rocks, and mixed soils. He is a pioneer in modeling granular micromechanics and has authored more than 300 papers in journals, edited books, and conference proceedings. He also serves as a reviewer for multiple journals, extramural funding agencies, and provides consulting services to the industry.

Jason Chao is a Ph.D. candidate in Geotechnical Engineering at the University of Massachusetts, Amherst, starting his program in 2021. Jason is committed to advancing geotechnical engineering knowledge through both experimental and theoretical approaches.

Prof. Yibing Deng is a Professor at Shanghai Urban Construction Vocational College. He earned his doctoral degree in geotechnical engineering from the University of Massachusetts Amherst in 2021. His research focuses on the effects of particle size distribution on the density state and shear behavior of granular soils, and he has developed several theoretical models to account for the influence of density state on mechanical behaviors. He has published over 40 articles in peer-reviewed journals.